Statistical Models for Ensemble Control by Alloying and Poisoning of Catalysts

II. Comparisons with Monte Carlo Simulations and with Experimental Results

I. ALSTRUP* AND N. T. ANDERSEN†

Haldor Topsøe Research Laboratories, DK-2800 Lyngby, Denmark; and † Mathematical Institute, University of Århus, DK-8000 Århus C, Denmark

In Part I (*J. Catal.* **104**, 454 (1987)) a new statistical poison lattice model (PLM) and short-range interaction model (SRIM) for calculation of the concentrations of various ensembles of active atoms or sites on partly passivated surfaces were derived. In the present paper examples of these models are compared with the concentrations of ensembles calculated by Monte Carlo simulation (MCS) of the deposition of the passivating atoms. Deposition of immobile (MCSIM) as well as mobile (MCSMO) atoms is simulated. The SRIM results are in complete agreement with the MCSIM results, while the PLM results are in good agreement with MCSMO results for ensembles containing three or more sites, while for single sites and pairs of sites significant differences are found. Experimental results for the initial sticking coefficients of H_2 and CO on Ni(100) surfaces with precoverage of sulfur are compared with PLM expressions and with Monte Carlo simulations. Experimental results for the sulfur precoverage dependence of the methanation rate on a nickel single crystal surface and on supported nickel catalysts are also compared with theoretical ensemble concentration values. Particle size dependences of some rate results for supported nickel catalysts, assumed to be partly poisoned by chemisorbed, reactant molecules, and the theory used for the interpretation of the results are also discussed. © 1987 Academic Press, Inc.

I. INTRODUCTION

In the preceding paper (*1*) (hereafter referred to as Part I) it was argued that the modern understanding of chemisorption systems indicate that the classical rate expressions

$$r = r_0(1 - a\Theta) \tag{1}$$

or

$$r = r_0(1 - \Theta)^n, \tag{2}$$

where Θ is the coverage of the surface by passivating or inactive atoms is inadequate for the determination of the critical size of ensembles of surface atoms (or sites) on which the process takes place. The expressions (1) and (2) do not take into account the form of the ensembles or the ordering in the pattern of passivating atoms, shown by LEED observations, or that the passivating

atoms influence neighbor atoms out to a certain distance.

In Part I two models were suggested which provide new expressions for the concentration of various surface ensembles. The models take into account the specific form of the ensembles as well as a range of influence of the passivating atoms. In the first model, denoted PLM (poison lattice model), the passivating atoms are assumed to occupy at random the sites of a lattice, the unit cell of which is in accordance with LEED observations of the surface with the passivating atoms. In the second model, denoted SRIM (short-range interaction model), the passivating atoms occupy the sites of the clean surface at random but the short-range order inferred from the LEED observations is taken into account in the deposition process.

In Part I the mathematical assumptions

and derivations were presented, the method for generating PLM expressions for specific cases was indicated, and SRIM formulas for the concentrations of active sites and pairs of active sites were derived for a (100) surface of a cubic crystal on which the chemisorption of a passivating atom excludes the chemisorption of other passivating atoms on the nearest neighbor sites.

In the present paper PLM and SRIM expressions are compared with Monte Carlo simulations. Comparisons are also made with experimental chemisorption and reaction rate results for nickel surfaces partly passivated by sulfur atoms under ultrahigh-vacuum (UHV) conditions and under conditions like industrial ones. The application to some of the reaction rate results of an expression derived by Martin (2) is briefly discussed.

Martin et al. (3) recently derived a particle-size-dependent expression for the concentration of ensembles consisting of n free, adjacent metal atoms on a surface on which atoms are blocked at random. In the limit of large particles the coverage dependence becomes identical to that of expression (2). The theory of Martin et al. (3) and its application to the particle size dependences of the rates of some processes on nickel catalysts are discussed in Section 3.

As in Part I two different coverage parameters, Θ and Θ_p, are used. Θ is the average number Y of inactive or passivating surface atoms divided by the number N_M of atoms in a complete surface layer of the clean metal surface and Θ_p is Y/N_P, where N_P is the number of inactive or passivating atoms when they form a complete surface structure.

2. NUMERICAL EXAMPLES AND COMPARISONS WITH MONTE CARLO SIMULATIONS

2.1. Poison Lattice Model

The mathematical details of the PLM are given in Part I (1). Here it suffices to recall that the model consists of two lattices, (i)

an M-lattice, the sites of which represent the atoms or chemisorption sites of the clean metallic catalyst surface, and (ii) a P-lattice, the sites of which represent possible sites for the deposition of passivating or inactive atoms.

The general expression for the concentration p_Ω of active ensembles of shape Ω was shown in Part I to be

$$p_\Omega = \sum_k q_k (1 - \Theta_p)^k, \qquad (3)$$

where q_k is the probability that the exposure number of an ensemble of shape Ω selected at random is k.

Three types of PLMs with different relations between the M-lattice with the points of the ensembles and the P-lattice with the passivating atoms are considered:

(i) Models with identical M- and P-lattices are called alloy models and are denoted $A(*, R)$.

(ii) Models with coincident M- and P-lattices but with a P-lattice unit cell larger than that of the M-lattice are called site passivation models and are denoted $PS(*, R, Z)$ (points of the P- and the M-lattices are hollow sites between the metal atoms).

(iii) Models where the P-lattice is part of or equal to the dual lattice of the M-lattice are called atom passivation models and are denoted $PA(*, R, Z)$ (points of the M-lattice are metal atom positions, while points of the P-lattice are hollow sites between metal atoms).

The asterisk (*) is H for hexagonal models and S for models with square lattices, R is the passivation range measured in unit of nearest neighbor distance, and $Z = N_M/N_P$.

The parameters of expression (3), i.e., the exposure numbers k and the exposure probabilities q_k, are shown for $A(S, R)$ and $A(H, R)$ in Tables 1 and 2, respectively, for a number of different ensembles.

Edge and corner effects can also be taken into account in PLMs and the contributions of active ensembles with edge lattice points are shown for the cases of the finite $M \times M$

TABLE I

Exposure Numbers k and Probabilities q_k for the $A(S, R)$ PLM (Finite $M \times M$ Lattice)

	Ensemble form									
	O		OO		OOO		88		888	
R	k	q_k	k	q_k	k	q_k	k	q_k	k	q_k
0	1	1	2	1	3	1	4	1	6	1
1	5	$(M-4)/M$	8	$(M-4)/M$	11	$(M-4)/M$	12	$(M-4)/M$	14	$(M-4)/M$
	4	$4/M$	7	$2/M$	10	$2/M$	10	$4/M$	12	$2/M$
			6	$2/M$	8	$2/M$			11	$2/M$
$\sqrt{2}$	9	$(M-4)/M$	12	$(M-4)/M$	15	$(M-4)/M$	16	$(M-4)/M$	20	$(M-4)/M$
	6	$4/M$	9	$2/M$	12	$2/M$	12	$4/M$	16	$2/M$
			8	$2/M$	10	$2/M$			15	$2/M$

atom square lattice and a regular hexagon with M atoms along an edge. The contribution from ensembles with corner lattice points is not shown, but is easily calculated. Edge and corner effects are illustrated in the example discussed in Part I.

It is seen that for large single crystal domains with negligible edge contributions expression (3) contains only one term for all alloy models. However, the meaning of the exponent k is for $R > 0$ different from the exponent n in the classical expression (2).

Exposure numbers, k, and probabilities q_k for the infinite models $PS(S, R, Z)$, $PS(H, R, S)$, $PA(S, R, Z)$, and $PA(H, R, Z)$ are shown in Tables 3, 4, 5, and 6, respectively, for a number of different ensembles. For these models expression (3) can contain more than one term even for the infinite lattice; e.g., it is seen that for ensembles consisting of three atoms forming a triangle on a hexagonal lattice the following expression is valid for the $PA(H, \sqrt{7}/\sqrt{3}, 4)$ model:

TABLE 2

Exposure Numbers k and Probabilities q_k for the $A(H, R)$ PLM (Regular Hexagon with $6M$-6 Edge Atoms)

	Ensemble form									
	O		OO		△		88		hex	
R	k	q_k	k	q_k	k	q_k	k	q_k	k	q_k
0	1	1	2	1	3	1	4	1	7	1
1	7	$(M-2)/M$	10	$(M-2)/M$	12	$(M-2)/M$	14	$(M-2)/M$	19	$(M-2)/M$
	5	$2/M$	8	$4/3M$	10	$1/M$	11	$2/M$	16	$2/M$
			7	$2/3M$	9	$1/M$				
$\sqrt{3}$	13	$(M-4)/M$	18	$(M-4)/M$	21	$(M-4)/M$	24	$(M-4)/M$	31	$(M-4)/M$
	12	$2/M$	17	$4/3M$	20	$1/M$	22	$2/M$	29	$2/M$
	8	$2/M$	16	$2/3M$	19	$1/M$	17	$2/M$	24	$2/M$
			13	$4/3M$	16	$1/M$				
			11	$2/3M$	14	$1/M$				

TABLE 3

Exposure Numbers k and Probabilities q_k for the PS(S, R, 2) PLM (Infinite Lattice)

	+		++		+++		⊞		⊞⊞	
R	k	q_k	k	q_k	k	q_k	k	q_k	k	q_k
0	0	1/2	1	1	1	1/2	2	1	3	1
	1	1/2			2	1/2				
1	1	1/2	4	1	4	1/2	6	1	8	1
	4	1/2			7	1/2				
$\sqrt2$	4	1/2	6	1	7	1/2	8	1	10	1
	5	1/2			8	1/2				

TABLE 5

Exposure Numbers k and Probabilities q_k for the PA(S, R, 2) PLM (Infinite Lattice)

	○		○○		○○○		⊙⊙		⊙⊙⊙	
R	k	q_k	k	q_k	k	q_k	k	q_k	k	q_k
$\sqrt2/2$	2	1	3	1	4	1	4	1/2	6	1
							5	1/2		
$\sqrt5/2$	6	1	8	1	10	1	9	1/2	13	1
							12	1/2		
$3/\sqrt2$	8	1	10	1	12	1	12	1/2	15	1
							13	1/2		

$$p = \tfrac{1}{8}[(1 - 4\Theta)^3 + 3(1 - 4\Theta)^4 + 3(1 - 4\Theta)^5 + (1 - 4\Theta)^7]. \quad (4)$$

The determination of the exposure number k is indicated in Fig. 1, in which the P atoms passivating various ensembles in the PA(S, $\sqrt2/2$, 2) model are shown. It is seen that ensembles consisting of singletons, pairs, and three atoms in a row have only one k value, viz., $k = 2$, 3, and 4, respec-

tively, while 2 × 2 ensembles have either $k = 4$ or $k = 5$ and with equal probability.

2.2. Comparisons between PLM, SRIM, and Monte Carlo Simulations

The relative concentration of active single sites as a function of Θ calculated using the expression for the PS(S, 1, 2) model and the SRIM expression for the concentration of singletons is shown in Fig. 2a together with the results of the Monte Carlo simula-

TABLE 4

Exposure Numbers k and Probabilities q_k for the PS(H, R, 3) PLM (Infinite Lattice)

	△		⋈		⋀		⋀⋁		✳	
R	k	q_k	k	q_k	k	q_k	k	q_k	k	q_k
0	0	5/6	0	2/3	0	1/3	0	1/3	1	2/3
	1	1/6	1	1/3	1	2/3	1	2/3	3	1/3
$1/\sqrt3$	0	1/3	1	1	1	2/3	1	1/3	1	1/3
									3	1/3
	1	2/3			3	1/3	2	2/3	4	1/2
1	1	2/3	1	1/3	1	1/6	3	2/3	4	1/2
					3	1/3			6	1/3
	3	1/3	3	2/3	4	1/2	4	1/3	7	1/6
$2/\sqrt3$	2	2/3	2	1/3	3	1/3	3	1/3	6	5/6
	3	1/3	3	2/3	4	2/3	4	2/3	7	1/6

TABLE 6

Exposure Numbers k and Probabilities q_k for the PA(H, R, 4) PLM (Infinite Lattice)

	○		○○		⊙⊙		⊙⊙		⊙⊙⊙	
R	k	q_k	k	q_k	k	q_k	k	q_k	k	q_k
$1/\sqrt3$	0	1	1	3/4	1	1/2	1	1/4	3	1
					2	3/8	2	1/2		
	1	3/4	2	1/4	3	1/8	3	1/4		
$2/\sqrt3$	1	3/4	1	1/4	1	1/8	3	3/4	3	1/4
	2	1/4								
	3	1/4	3	1/2	3	3/8	4	1/4	5	3/4
$\sqrt7/\sqrt3$	3	1	3	1/4	3	1/8	4	1/4	6	1/4
			4	1/2	4	3/8	5	1/2	7	3/4
			5	1/4	5	3/8	7	1/4		
					7	1/8				

PLM   PA (S,$\frac{\sqrt{2}}{2}$, 2)

▨ atom site of ensemble

o possible site of passivating atom

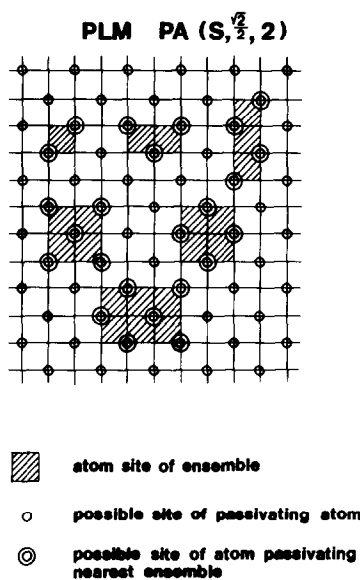◎ possible site of atom passivating
    nearest ensemble

FIG. 1. Various metal atom ensembles on a square lattice with passivating atoms forming a $c(2 \times 2)$ structure. The atoms passivating the ensembles when $R = \sqrt{2}/2$ are indicated.

tions. Figure 2b shows the concentration of pairs of active sites for the same models and simulations. Results from two types of Monte Carlo simulation are shown. In both types the same nearest neighbor rules are obeyed as in the PS(S, 1, 2) PLM and in the SRIM; i.e., sites which are nearest neighbors to sites occupied by passivating atoms cannot be occupied. In the type denoted MCSIM, sites of a square lattice selected by a random number generator are blocked and the nearest neighbor sites are passivated if the site selected is active, i.e., not previously blocked or passivated. When the number of blocked sites corresponds to the specified coverage the process is stopped and the number of free sites and pairs of free sites is counted. In the other type, denoted MCSMO, a random walk is commenced on the lattice if the selected site is not active. The random walk is continued until an active site is found. The first type is thus simulating immobile chemisorption of the passivating atoms while the second type is simulating chemisorption with a mobile precursor. The short-range

order obtained in the chemisorption pattern is in both cases the same as in the $c(2 \times 2)$ structure on a (100) surface of a cubic crystal. The simulations have been made for a square lattice with 100×100 sites using periodic boundary conditions.

Within the accuracy of the simulations the MCSIM and the SRIM results are equal, indicating the high accuracy of the approximate SRIM formulas:

$$p_s \simeq (1 - \Theta) \left(\frac{1 - 2\Theta}{1 - \Theta}\right)^4 \tag{5}$$

$$p_d \simeq (1 - \Theta) \left(\frac{1 - 2\Theta}{1 - \Theta}\right)^5 \frac{1}{\left(1 + \frac{(1 - \Theta)\Theta}{(1 - 2\Theta)^2}\right)^2} \tag{6}$$

derived in Part I. p_s is the concentration of active single sites and p_d the concentration of pairs of active sites.

At high coverages the concentration of active single sites as calculated using the PLM formula

$$p_s = \frac{1}{2}[(1 - 2\Theta) + (1 - 2\Theta)^4] \tag{7}$$

is significantly higher than the simulation results while the concentration of pairs of active sites calculated using the PLM formula

$$p_d = (1 - 2\Theta)^4 \tag{8}$$

is somewhat lower than the MCSMO results.

PLM results for the same model but for larger ensembles are compared with MCSMO results in Fig. 2c. It is seen that the two types of calculations give almost the same results for these larger ensembles (while MCSIM gives significantly lower concentrations). The differences in the patterns of passivating atoms in the two types of simulations are indicated in Fig. 3. As could be expected, the atoms are more evenly distributed in the MCSIM than in the MCSMO calculation. In the latter case more extended domains with $c(2 \times 2)$ structure as well as larger islands of free sites are seen.
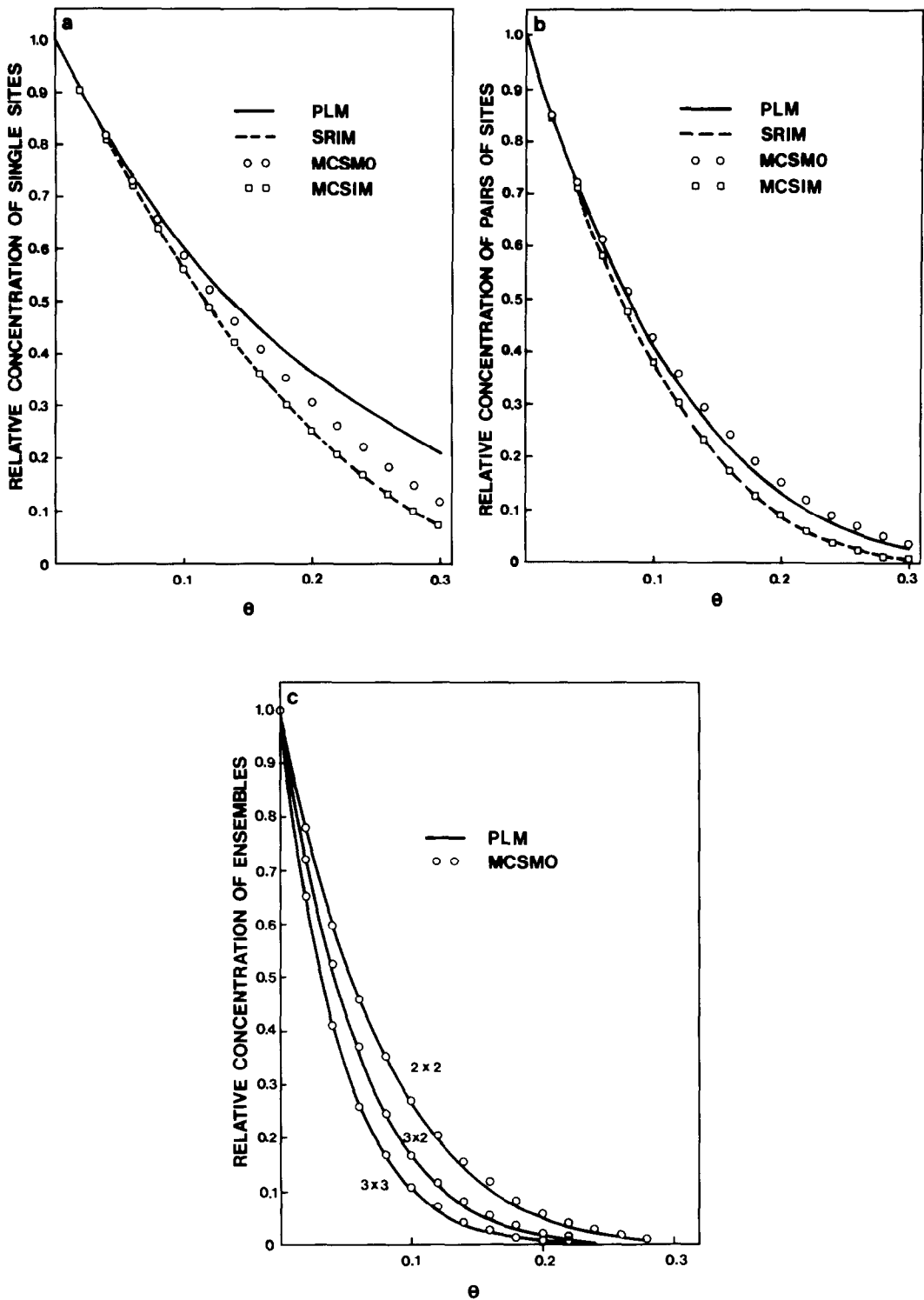
FIG. 2. Relative concentration of various ensembles of active sites as function of the coverage Θ of passivating atoms in the PS(S, R, 2) PLM and in the corresponding SRIM compared with Monte Carlo simulations: (a) single sites; (b) pairs of sites; (c) 2×2, 3×2, and 3×3 ensembles.
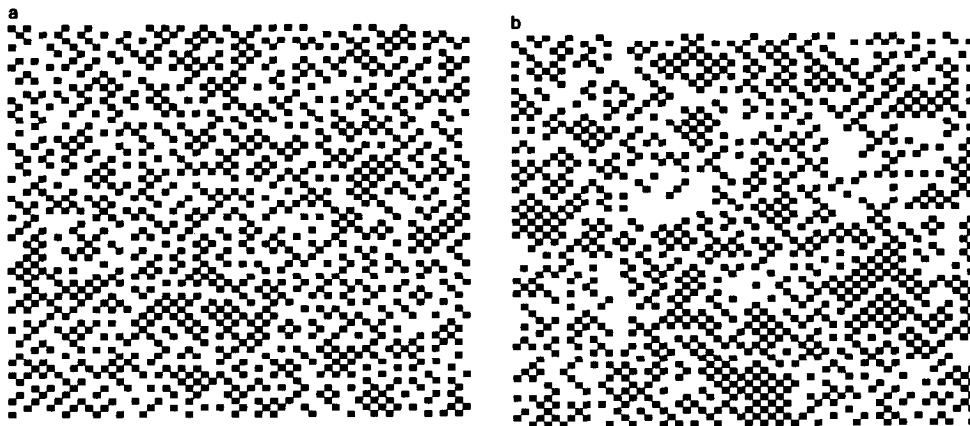
FIG. 3. Monte Carlo simulations of the chemisorption on a square lattice of atoms, which excludes chemisorption on neighbor sites, for $\Theta = 0.3$: (a) immobile chemisorption (MCSIM); (b) mobile precursor (MCSMO).

Similar Monte Carlo simulations were made corresponding to a passivation range equal, as above, to the nearest neighbor distance but with a short-range order corresponding to the one in the $p(2 \times 2)$ structure on the (100) surface of a cubic crystal; i.e., the passivating atoms prevent the chemisorption of other passivating atoms on the nearest and next nearest neighbor sites. These results are compared with experimental results in Section 3.

3. DISCUSSION AND COMPARISONS WITH EXPERIMENTS

Of the two models, the PLM and the SRIM, suggested in Part I, only the latter corresponds to a physically probable chemisorption process for the passivating atoms; viz., if the atom approaching the surface from the gas phase hits an unoccupied site with unoccupied neighbor sites it is chemisorbed on that site and cannot move on the surface, but if these conditions are not fulfilled then the atom returns to the gas phase. The formulas (5) and (6) are approximate but the comparisons with the Monte Carlo simulations show that they are very accurate. The disadvantage of the SRIM is that it is not in accordance with the long-range order observed by LEED.

Introduction of surface mobility of the adsorbing species before they are fixed on a surface site, i.e., assuming that the chemisorption takes place through a mobile precursor, may enhance the growth of domains with sufficient long-range order for the formation of a LEED pattern, as indicated in Fig. 3. The effect of precursor mobility on the SRIM is significant for the concentrations of active single sites and pairs of active sites but small for ensembles containing more than two atoms or sites.

The PLM, on the other hand, is at saturation in accordance with the observed long-range order. However, it is unphysical in that it excludes all sites not on the P-lattice as possible chemisorption sites for the passivating atoms. The error due to this artificial rule is, as mentioned in Part I, expected to be small at low as well as at high P-lattice coverages. The comparisons between the Monte Carlo simulations with mobile precursor and the PLM show good agreement for larger ensembles (Fig. 2c). The single site PLM curve is, however, significantly below the MCSMO curve but somewhat above the MCSIM curve (Fig. 2a). The pair PLM curve, on the other hand, is slightly above the MCSMO curve (Fig. 2b).

3.1. Sulfur Poisoning of Chemisorption and Catalytic Reactions

Much work has been devoted to the study of the influence of chemisorbed sulfur

on the catalytic activity of metal catalysts and in particular nickel catalysts (4), not only due to its importance as a severe poison but also as a means of changing the selectivity of catalytic reactions. Also the chemisorption of sulfur on nickel and nickel catalysts has been studied by many workers (4). However, due to considerable experimental difficulties only a few studies have provided thermodynamic information (5, 6).

LEED studies at room temperature of Ni(100) surfaces dosed with sulfur at very low pressure show the formation of an ordered $p(2 \times 2)$ surface structure up to $\Theta = 0.25$ and from $\Theta = 0.25$ to $\Theta = 0.5$ an ordered $c(2 \times 2)$ surface structure (4). The adsorption of sulfur on Ni(110) and Ni(111) is more complicated. At low sulfur coverage and below 400 K a $p(2 \times 2)$ structure is formed on Ni(111) up to about $\Theta = 0.31$ (4). At higher temperatures the diffraction pattern is reversibly transformed into one with the same symmetry as seen for the clean surface, i.e., a $p(1 \times 1)$ structure (7). At higher coverages a $p(\sqrt{3} \times \sqrt{3}) - 30°$ is formed at low temperature, but at room temperature and upward (up to about 600 K) a more complex pattern is seen. The interpretation of this complex pattern is controversial. Edmonds et al. (8) and Perdereau and Oudar (9) interpreted it in terms of reconstruction of the surface, while Erley and Wagner (10) explained it in terms of a coincidence net, $c(20 \times 2)$, produced by a closed packed sulfur overlayer on the Ni(111) surface. Above about 700 K a $p(1 \times 1)$ structure is formed also at high coverages. The transformation was observed to be reversible also in the high coverage range ($0.33 < \Theta < 0.5$) but some hysteresis was seen (7).

One of the difficulties besetting the determination of the chemisorption thermodynamics of sulfur on transition metal surfaces is that very small H_2S/H_2 ratios are required to obtain equilibrium with the chemisorbed layer of sulfur; e.g., a H_2S/H_2 ratio equal to 10 ppb corresponds at 650 K

to a coverage greater than 80% of the saturation. Recent studies (5, 6) show that the heat of chemisorption of H_2S on supported nickel catalysts in the temperature range 800–1100 K decreases linearly with increasing sulfur coverage at least in the range from about 0.6 to 1.0 of the saturation, which indicates a strong interaction between the chemisorbed sulfur atoms.

Kiskinova and Goodman (11) studied the influence of preadsorbed S (as well as preadsorbed Cl and P) on the chemisorption of H_2 and CO on a Ni(100) surface at 100 K. From the data obtained they calculated the initial sticking coefficients of H_2 and CO molecules as functions of the sulfur coverage. At sulfur coverages $\Theta \leq 0.25$ it is known, as mentioned above, that sulfur atoms arrange themselves in a $p(2 \times 2)$ structure on the Ni(100) surface. Results indicate that sulfur has a passivation range for CO chemisorption which is smaller than the next nearest neighbor distance because the initial sticking coefficient of CO is appreciable at $\Theta = 0.25$. In Fig. 4 the initial sticking coefficients obtained by Kiskinova and Goodman are plotted as functions of the sulfur coverage together with the curves corresponding to the concentrations of active single sites (singletons) and active pairs of sites when the position of sulfur is assumed to be in accordance with the $p(2 \times 2)$ structure and the passivation range is assumed to be equal to the nearest neighbor distance.

Under these conditions the poison lattice model gives the following expression for the relative concentration of singletons

$$p_s = \tfrac{1}{4}[1 + (1 - 4\Theta) + 2(1 - 4\Theta)^2], \quad (9)$$

while the concentration of pairs is given by

$$p_d = (1 - 4\Theta)^2. \quad (10)$$

Curves for the concentrations of singletons and pairs as determined by Monte Carlo calculations are also shown. The solid lines correspond to immobile adsorption of the sulfur atoms; i.e., if the site selected at random is occupied or has nearest or next
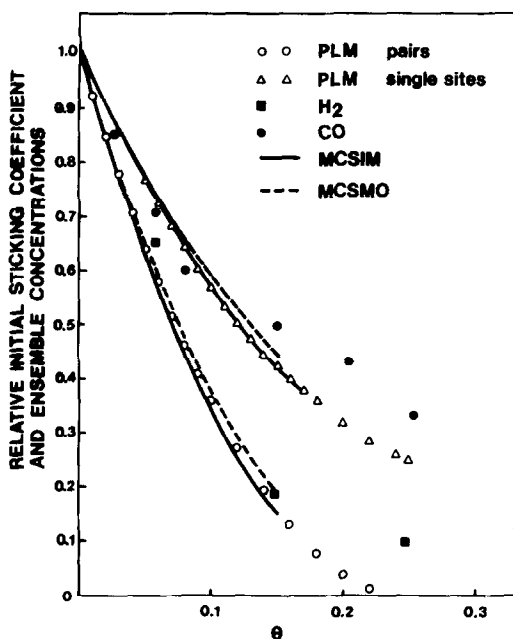
FIG. 4. Experimental initial sticking coefficients of H_2 and CO on a Ni(100) surface as a function of sulfur coverage Θ (from Ref. (11)) compared with PLM and Monte Carlo calculations.

nearest neighbor sites occupied then no adsorption takes place in this attempt. The broken lines correspond to mobile sulfur adsorption; i.e., if the adsorption attempt on the randomly selected site is not successful, then a site fulfilling the conditions for adsorption is found by moving around on the surface in a random way. The passivation range for the ensembles is, however, equal to the nearest neighbor distance.

It is seen that assuming mobile adsorption increases the singleton and pair concentrations, but only by a small amount, and that the poison lattice model gives concentrations between those calculated by immobile and mobile Monte Carlo simulations. The experimental points for the initial sticking coefficients of H_2 an CO as functions of the sulfur coverage are in quite good agreement with the concentrations of pairs and singletons, respectively, especially at low sulfur concentrations. At higher sulfur concentrations it is seen that the experimental sticking coefficients are

somewhat larger than the theoretical ensemble concentration values. Especially in the case of CO, the sticking coefficient drops very little in the sulfur coverage range $0.1 < \Theta < 0.18$. This plateau, which is even more pronounced in the case of Cl poisoning, indicates that the sticking mechanism changes when the coverage of the poisoning atoms approaches that at which transition from the $p(2 \times 2)$ to the $c(2 \times 2)$ structure takes place.

It may be speculated that higher sulfur mobility is present in this coverage region and that the impinging CO molecules are able to displace the sulfur atoms and compress the sulfur surface structure as has been reported for the Ni(111) surface by Erley and Wagner (10). This change is also reflected in the fact that the thermal desorption spectrum of CO changes as a function of sulfur coverage from being dominated by β-CO with a desorption temperature of ca. 500 K at low coverages to increasingly being dominated by α-CO with a desorption temperature of about 300 K. At about $\Theta = 0.25$ the β-peak has disappeared completely.

Recent theoretical studies (12) of the influence of adsorbed electronegative atoms on the electronic properties of metal surfaces indicate that the models described in the present paper could be made more realistic by replacing the passivation range by a distance-dependent passivation strength. The PLM can, as briefly mentioned in Part I and indicated in expressions A8 and A9 of Appendix A of Part I, be easily generalized in this direction. The fact that the experimental sticking probability falls off more rapidly with Θ at small Θ than the PLM curve in Fig. 4, and also that this deviation is more pronounced for passivation by the more electronegative Cl atoms (11), would be in accordance with such an improved model. The problem with this generalization is, of course, the difficulty in independently determining the values of the new parameters introduced.

The corresponding sticking coefficient

results for Ni(100) precovered with phosphorus are very different with a much weaker coverage dependence. This may be explained by the fact that the LEED studies indicate strong island formation or the formation of an amorphous Ni–P surface compound, as they showed no ordered structure (11).

Goodman and Kiskinova (13) also investigated the influence of preadsorbed sulfur on the methanation reaction and their results are shown in Fig. 5 for a pressure of 120 Torr, $H_2/CO = 4/1$, and a reaction temperature = 600 K. It is seen that the drop in the methanation rate with sulfur coverage is very large at small sulfur coverages. Application of the simple expression (2) to the data predicts that very large ensembles containing about 30 Ni atoms are necessary for the reaction. If instead it is assumed that the sulfur atoms are arranged in accordance with the $p(2 \times 2)$ structure and that the passivation range includes next nearest neighbor sites, then the drop in the methanation

FIG. 5. Experimental rates of methanation on a Ni(100) surface as a function of sulfur coverage Θ (from Ref. (13)) compared with PLM and Monte Carlo calculations.

rate corresponds well to the drop in the concentration of ensembles containing $5 \times 3 = 15$ active sites, as can be seen from Fig. 5 where the concentration of 5×3 ensembles calculated by Monte Carlo simulation and by using the expression

$$r/r_0 = \tfrac{1}{6}[2(1 - 4\Theta)^{12} + 2(1 - 4\Theta)^9 + (1 - 4\Theta)^8 + (1 - 4\Theta)^6], \quad (11)$$

derived using the poison lattice model, is shown.

In a few papers (14, 15) investigations of the dependence on sulfur poisoning of the rate of methanation on nickel catalyst has been reported for conditions similar to industrial ones. Fitzharris et al. (14) concluded from their measurements that the methanation rate as a function of sulfur coverage Θ follows the expression

$$r/r_0 = (1 - 2\Theta)^2 = (1 - \Theta_p)^2, \quad (12)$$

in strong contradiction to the above-mentioned results of Goodman and Kiskinova (13). The results of Fitzharris et al. (14) were obtained using a constant feed by monitoring the methane and H_2S concentrations of the gas from the outlet of the reactor during the transient period before steady state was reached. The time-dependent sulfur surface concentration of the catalyst was calculated by integrating the difference between the H_2S concentrations of the feed gas and the outlet gas corresponding to various times during the transient period. Only the results of the analysis of transients corresponding to 55 ppb H_2S in the feed were reported. However, if the curves reported for the transient observed with 15 ppb H_2S in the feed are analyzed in the same way then, as shown in Fig. 6, results are obtained which indicate a stronger drop in the methanation activity at small sulfur concentrations and these results are not in contradiction with the results of Goodman and Kiskinova. A nonuniform deposition of sulfur on the nickel catalyst surface during the 55 ppb transient could explain the discrepancy.
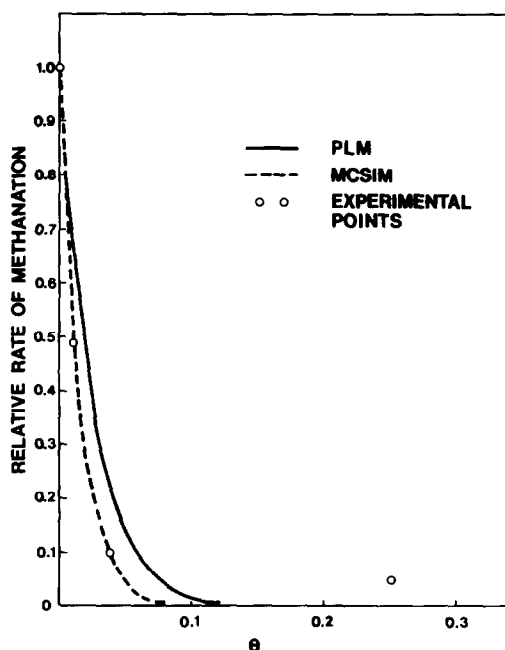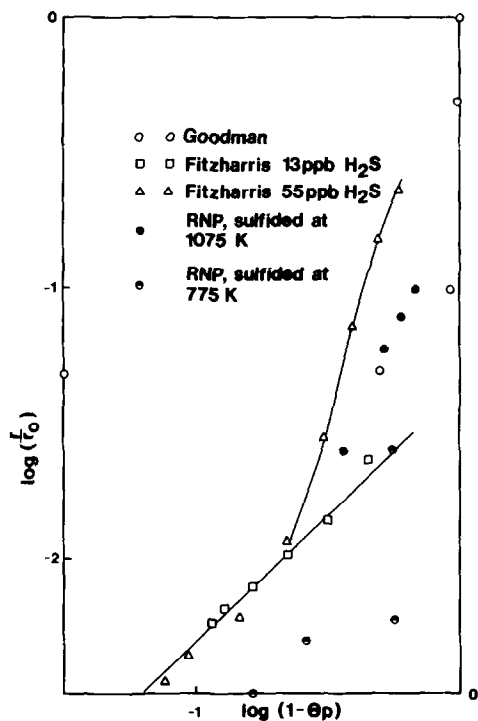
FIG. 6. Rates of methanation on alumina-supported nickel catalysts as a function of sulfur coverage (from Fitzharris et al., (14) and from RNP (15)) compared with the results of Goodman and Kiskinova for a sulfur-passivated Ni(100) surface (ref. (13)).

Rostrup-Nielsen and Pedersen (RNP) (15) measured the methanation activity in differential reaction studies for 25% Ni/Al$_2$O$_3$ catalysts presulfided at 575, 775, and 1075 K with H$_2$S/H$_2$ varied between 8.4 ppb and 5.7 ppm. Their results were fitted to the classical expression $r/r_0 = (1 - \Theta_p)^n$, resulting in $n \simeq 4.3$. However, the results invite another interpretation which is in much better agreement with the results of Goodman and Kiskinova (13).

The points corresponding to sulfidation at 1075 K fit very well with a straight line which is not going through the point corresponding to the activity of the sulfur-free catalyst, but with $n \simeq 2$. The same seems to be true for the points corresponding to presulfidation at 775 K, but in this case the line corresponds to lower activities, indicating an uncertainty in the normalization of the group of activities corresponding to one

sulfidation temperature. With this interpretation the group of points corresponding to sulfidation at 1075 K and similarly the group for 775 K sulfidation separately are in agreement with the heavy drop in methanation activity observed by Goodman and Kiskinova. The points of RNP (15) are also shown in Fig. 6.

Recently Martin (2) suggested the following expression for the calculation of the concentration of active square ensembles on a (100) surface of a cubic crystal:

$$\ln p_x = \ln(1 - \Theta_p) - \gamma - 2\sqrt{\gamma} \sqrt{-\ln(1 - \Theta_p)}. \quad (13)$$

p_x is the probability that a square ensemble with x atoms is active on a surface with p square islands with poison atoms. Θ_p is the poison atom coverage of the surface, and $\gamma = px/N$, where N is the total number of surface metal atoms.

Expression (13) was compared with some of the methanation rate values measured by RNP and good agreement was obtained. This apparent confirmation of the theory requires some comments:

(i) Only 4 out of the 10 experimental points presented by RNP were used in the comparison. The 6 missing points are not in agreement with the same theoretical curve.

(ii) It is important to realize that the determination of the sulfur coverages is inaccurate due to the difficulty mentioned above of measuring very small H$_2$S concentrations in the gas phase.

(iii) Expression (13) gives wrong results at small poison coverages, i.e., at coverages where methanation rates corresponding to accurate sulfur coverages, determined by Auger electron spectroscopy, are available in the work of Goodman and Kiskinova (13). According to (13) $p_x = \exp(-\gamma)$ for $\Theta_p = 0$, while the true value is 1. The fit to the four RNP points selected by Martin (2) gives $\gamma = 0.8$; i.e., $p_x = 0.45$ for $\Theta_p = 0$. In the range of small coverages where the poison islands do not yet overlap, γ cannot be considered a constant as

the concentration of ensembles should simply be proportional to $1 - \Theta_p$.

The theory of Martin may provide an interesting alternative possibility of explaining the coverage dependence of the concentration of active ensembles at high poison coverages. Experimental results in this range are, however, not reliable enough to allow an evaluation of the theory. At small sulfur coverages the island growth model cannot explain the strong drop in the methanation activity observed by Kiskinova and Goodman.

3.2. Particle Size Dependence of Self-Poisoning

Martin et al. (3) derived the following expression for the probability P that a selected ensemble consisting of x adjacent surface metal atoms is free from adspecies on a surface consisting of N metal atoms, q of which are covered by passivating adspecies:

$$P = \frac{\binom{N - x}{q}}{\binom{N}{q}}. \qquad (14)$$

They used the N-dependence of (14) to explain the observed particle size dependences of the rate of hydrogen–deuterium exchange of methane (16) and of the rate of ethane hydrogenolysis (17) on silica-supported nickel catalysts. The passivating adspecies were assumed to be reactant atoms or molecules.

In the theory of Martin et al. (3) only the metal atom on which the passivating atom or molecule is chemisorbed is assumed to be passivated. The relative number of active ensembles should not, however, as discussed in Part I, depend on the size of the metal lattice when the passivation takes place through blocking only. If the adspecies are passivating neighbor metal atoms or sites also, then the relative concentration of active ensembles depends on the size of the metal surface, i.e., on the metal particle

size of the catalyst. This size dependence is, however, opposite to that observed in the above examples because the probability of ensemble passivation is smaller for ensembles near the edges of the surface than for ensembles far from the edges.

The erroneous size dependence of (14) is due to the unphysical assumption that the number q of adspecies is assumed to be the same for all the metal surfaces (assumed to contain N metal surface atoms). Experimentally it is of course impossible to control the coverage of the individual catalyst metal particles, so q has to be treated as a random variable with a mean value equal to $\Theta \cdot N$, where Θ is the observed coverage of adspecies for the catalyst sample.

Thus the expression (14) is not applicable to the individual particles but can be applied to the entire sample. N means then the sum of all the surface metal atoms of the sample and q is equal to $\Theta \cdot N$, where Θ is the observed poison coverage. N is typically of the order of 10^{20} per gram of catalyst; i.e., the difference between (14) and the limit value $(1 - \Theta)^x$ for $N \to \infty$ is negligible, which clearly shows that the ensemble concentration does not depend on the particle size. This result is in agreement with the PLM alloy models for $R = 0$.

Also another shortcoming of expression (14) makes it inapplicable to a discussion of the particle size dependence of ensemble-controlled reactions. It does not take into account the form of the metal surface and the form of the ensembles. The number of active ensembles per unit metal area and its dependence on particle size cannot be calculated. It is obvious, however, that if the metal area is not very much larger than the ensembles the number of ensembles per unit metal area decreases significantly when the particle size is decreased. This particle size dependence can be calculated by using the PLM described in Part I.

However, as detailed knowledge of the particle size distribution and the sizes and orientation of the surface planes of the particles is not available, the particle size de-

pendence of the reaction rate can probably not provide a reliable determination of the size and shape of the controlling ensembles.

The discussion below should therefore be considered only as a qualitative illustration of the influence of the finite size of the particles on the number of ensembles per unit surface area.

If it is assumed that the metal particles are cubooctahedra (3), the relation between the particle diameter D and the number M of metal atoms along the edges of the square faces is given by

$$D = 2(M - 1)d, \qquad (15)$$

where d is the diameter of the metal atoms.

The number N_E of ensembles on the square face with $M \times M$ metal atoms is given by (18).

$$N_E = 2(M - r + 1)(M - s + 1) \quad (16)$$

when the active ensembles are assumed to be rectangles consisting of $r \times s$ metal atoms.

If it assumed that the particle size dependence (16) of the number of ensembles on the square faces is representative for the total surface of the particles, then the reaction rate per unit metal area relative to the rate for large particles is approximately given by

$$r_M/r_\infty = \left(1 - \frac{r - 1}{M}\right)\left(1 - \frac{s - 1}{M}\right). \quad (17)$$

With $r = 2$ and $s = 1$, relative rates calculated using (17) are in good agreement with the experimental results for CD_4 formation (16), and the rate data for ethane hydrogenolysis (17) are in good agreement with the relative rates calculated from (17) assuming $r = 3$ and $s = 1$. These small ensembles are in contrast to the very large ensembles (15 and 24 atoms, respectively, for the above two processes) calculated by Martin et al. (3) on the basis of (14).

4. CONCLUSIONS

Although the assumption of the poison lattice model that the passivating atoms occupy the sites of a rigid lattice seems unrealistic, the model gives good agreement with Monte Carlo simulations. The comparisons indicate that the agreement is particularly good for ensembles consisting of more than two atoms or sites.

The interpretation, using PLM and MCSIM, of the sulfur coverage dependence of the methanation rate on Ni(100) with low coverage of sulfur indicates that 5×3 site ensembles are crucial for the process. Reinterpretations of methanation rates on sulfur-passivated, supported nickel catalysts at industrial conditions remove apparent conflicts with the single crystal results.

Finally the particle size dependences of H–D exchange and ethane hydrogenolysis on supported nickel catalysts, which was recently explained by an ensemble theory, is commented on.

Fair agreement is also obtained with the coverage dependence of experimental initial sticking coefficients for H_2 and CO on a sulfur-precovered Ni(100) surface, indicating that the chemisorption of a CO and an H_2 molecule requires one and two active sites, respectively.

More perfect agreement can be obtained if a generalized model with distance-dependent passivation strength is used, but this would require independent determination of the extra parameters introduced and the desirable simplicity of the model would be lost.

REFERENCES

1. Andersen, N. T., Topsøe, F., Alstrup, I., and Rostrup-Nielsen, J. R., J. Catal. 104, 454 (1987).
2. Martin, G. A., Surf. Sci. 162, 316 (1985).
3. Martin, G. A., Dalmon, J. A., and Mirodatos, C., in "Proceedings, 8th International Congress on Catalysis, Berlin, 1984," pp. IV-371. Verlag Chemie, Weinheim, 1984.
4. Bartholomew, C. H., Agrawal, P. K., and Katzer, J. R., in "Advances in Catalysis" (D. D. Eley, P. W. Selwood, and P. B. Weisz, Eds.), Vol. 31, p. 135. Academic Press, Orlando, FL, 1983.

5. McCarty, J. C., and Wise, H., *J. Chem. Phys.* **72**, 6332 (1980).

6. Alstrup, I., Rostrup-Nielsen, J. R., and Røen, S., *Appl. Catal.* **1**, 303 (1981).

7. Ramanathan, R., and Blakely, J. M., *Mater. Lett.* **2**, 12 (1983).

8. Edmonds, T., McCarroll, J. J., and Pitkethly, R. C., *J. Vac. Sci. Technol.* **8**, 68 (1971).

9. Perdereau, M., and Oudar, J., *Surf. Sci.* **20**, 80 (1970).

10. Erley, W., and Wagner, H., *J. Catal.* **53**, 287 (1978).

11. Kiskinova, M., and Goodman, D. W., *Surf. Sci.* **108**, 64 (1981).

12. Nørskov, J. K., Holloway, S., and Lang, N. D., *Surf. Sci.* **137**, 65 (1984).

13. Goodman, D. W., and Kiskinova, M., *Surf. Sci. Lett.* **105**, 265 (1981).

14. Fitzharris, W. D., Katzer, J. R., and Manogue, W. H., *J. Catal.* **76**, 369 (1982).

15. Rostrup-Nielsen, J. R., and Pedersen, K., *J. Catal.* **59**, 395 (1979).

16. Dalmon, J. A., and Mirodatos, C., *J. Mol. Catal.* **25**, 161 (1984).

17. Martin, G. A., and Dalmon, J. A., *J. Catal.* **75**, 233 (1982).

18. Miyazaki, E., and Yasumori, I., *J. Math. Phys.* **18**, 215 (1977).